https://doi.org/10.17221/78/2025-JFS

Tree-ring based climate reconstruction and growth–climate analysis of *Pinus kesiya* Royle ex Gordon in Doi Khuntan National Park, northern Thailand

Kritsadapan Palakit[1], *Khwanchai Duangsathaporn*[1], *Nathsuda Pumijumnong*[2], *Supasit Sriarkarin*[1], *Thanyaporn Bungbai*[1], *Pichit Lumyai*[1]*

[1]*Department of Forest Management, Faculty of Forestry, Kasetsart University, Bangkok, Thailand*
[2]*Faculty of Environment and Resource Studies, Mahidol University, Nakhon Pathom, Thailand*

**Corresponding author: fforpcl@ku.ac.th*

Citation: Palakit K., Duangsathaporn K., Pumijumnong N., Sriarkarin S., Bungbai T., Lumyai P. (2026): Tree-ring based climate reconstruction and growth–climate analysis of *Pinus kesiya* Royle ex Gordon in Doi Khuntan National Park, northern Thailand. J. For. Sci., 72: 174–187.

Abstract: Tree-ring analysis is a valuable tool for understanding long-term climate patterns and their influence on tree growth. This study investigates the climate–growth relationships of Khasi pine (*Pinus kesiya* Royle ex Gordon) in Doi Khuntan National Park, northern Thailand (at elevations of 850 to 1 035 m a.s.l.), to reconstruct past climate and inform forest management. Using 48 cross-dated increment cores, we developed an 83-year chronology (1936–2018). Standard dendrochronological methods and regression models were applied. The radial growth of *P. kesiya* was primarily influenced by moisture availability, showing significant positive correlations with March rainfall (r = 0.39, P < 0.01) and April–July relative humidity (r = 0.45, P < 0.01). Growth was negatively correlated with April–July mean temperature (r = –0.47, P < 0.01), indicating that warmer wet seasons induce stress. False-rings served as complementary intra-annual drought proxies, linked to cool-dry transitional periods. Multiple regression models explained 40.6% of radial growth variance and 65.6% of false-ring frequency variance. Reconstructed climate series revealed significant warming trends since the 1930s, most pronounced in April extreme minimum temperature, which increased by +0.98 °C over the study period (Mann-Kendall test, P < 0.01). These findings highlight the vulnerability of montane pine forests to increasing temperatures and atmospheric dryness, providing a multi–proxy baseline for climate change adaptation.

Keywords: dendrochronology; false ring; intra-annual ring; Khasi pine; montane forest

Climate change represents a major global threat to ecological systems, with montane forests being particularly vulnerable due to their adaptation to narrow climatic niches and limited altitudinal mobility (Feeley et al. 2012; Seidl et al. 2017; Vacek et al. 2023). In Southeast Asia, mean surface temperatures have risen approximately 0.14–0.20 °C per decade over the past

Supported by the Office of the Permanent Secretary, Ministry of Higher Education, Science, Research and Innovation (OPS MHESI), and Thailand Science Research and Innovation (TSRI) (Grant No. RGNS 63-043).

https://doi.org/10.17221/78/2025-JFS

50 years, accompanied by more frequent and intense droughts, heatwaves, and increasingly erratic monsoon patterns (IPCC 2022). These climatic shifts undermine the essential ecosystem services provided by montane forests, including carbon sequestration, watershed regulation, soil stabilisation, biodiversity conservation, and socio-economic benefits for local communities (Singh et al. 2021; Thammanu et al. 2021a).

In northern Thailand, natural pine forests dominated by Khasi pine (*Pinus kesiya* Royle ex Gordon) play a critical eco-functional and socio-economic role (Thammanu et al. 2020, 2021a). These forests form vital carbon sinks, stabilise erosive steep slopes, and regulate watershed hydrology essential for downstream agriculture (Khamyong, Anongrak 2016; Thammanu et al. 2021b). They also serve as refuges for endemic and threatened species and provide sources of non-timber forest products (Trisurat et al. 2015). However, these forests face escalating threats from altered rainfall patterns, prolonged droughts, and rising temperatures, which can disrupt growth cycles, enhance susceptibility to pests and disease, and reduce natural regeneration capacity (Rakthai et al. 2020; Marod et al. 2025). Observations of increasing pine mortality in Thailand's national parks raise critical questions about forest resilience to ongoing climate change (Temchai et al. 2018).

A primary challenge for adaptive management is the scarcity of long-term, high-resolution climate data for mountainous regions, which typically have fewer weather stations than lowland areas (Hofer, Horak 2020; Strachan et al. 2016). Most instrumental records span only a few decades, limiting analysis of longer-term climate patterns and variability. Tree-ring analysis (dendrochronology) provides a powerful tool to overcome this limitation, enabling high-resolution reconstructions of past climate that can span centuries through measurements of annual and intra-annual ring width and structure (Speer 2010). These paleoclimate records help identify both long-term climatic trends and short-term anomalies that influence tree growth and forest dynamics.

In subtropical and tropical forests, annual ring boundaries are often less distinct than in temperate regions, with a higher occurrence of false rings (intra-annual density fluctuations) due to temporary stress from drought or temperature changes (Palakit et al. 2012, 2015; Herrera-Ramirez et al. 2017). While complicating simple ring counts, false rings – once correctly identified – provide valuable additional information on intra-annual climate events not captured by annual rings alone (Pumijumnong, Palakit 2020). For *P. Kesiya*, recent studies have demonstrated their sensitivity to seasonal moisture and temperature variations (Palakit, Pumijumnong 2024; Thomte et al. 2022a, 2023), but comprehensive analyses integrating both standard ring-width and false-ring indices for a robust climate reconstruction remains limited.

The Doi Khuntan National Park, with its relatively undisturbed *P. Kesiya* stands at 1 000–1 300 m elevation, provides an ideal setting to examine these climate–growth relations. Located in a transition zone influenced by both southwest and northeast monsoons, the park's pine forests represents typical montane ecosystems of northern Thailand (Pumijumnong, Eckstein 2011). This study explicitly aims to: (*i*) analyse the annual and intra-annual (via false-ring frequency) growth–climate relationships of *P. kesiya*; (*ii*) assess the climatic drivers of false ring formation; and (*iii*) reconstruct the past climate trends using multi-proxy tree-ring data. By examining how intra-annual and seasonal climatic variables shape growth trends, with emphasis on false rings as proxy indicators of short-term climate variability, this research provides essential baseline information for forest conservation and management amidst ongoing and projected climate intensification (IPCC 2022).

MATERIAL AND METHODS

Study area. The study was conducted in Doi Khuntan National Park, Lamphun Province, northwestern Thailand [18°22'N – 18°37'N, 99°12'E – 99°25'E (Figure 1)]. The park features dense montane pine forests interspersed with mixed evergreen and deciduous species at elevations ranging from 850 m a.s.l. to 1 035 m a.s.l. According to the Köppen-Geiger classification system, the climate is tropical savanna (Aw), characterised by three distinct seasons: rainy season (May–October), winter season (November–February), and summer season (March–April) (Linasmita, Pumijumnong 2004). Temperatures range from approximately 38 °C maximum in summer to around 5 °C minimum in winter, with a mean annual rainfall of approximately 1 034 mm. Soils are predominantly sandy-loam soil, and the fire regime is characterised by low-intensity

https://doi.org/10.17221/78/2025-JFS

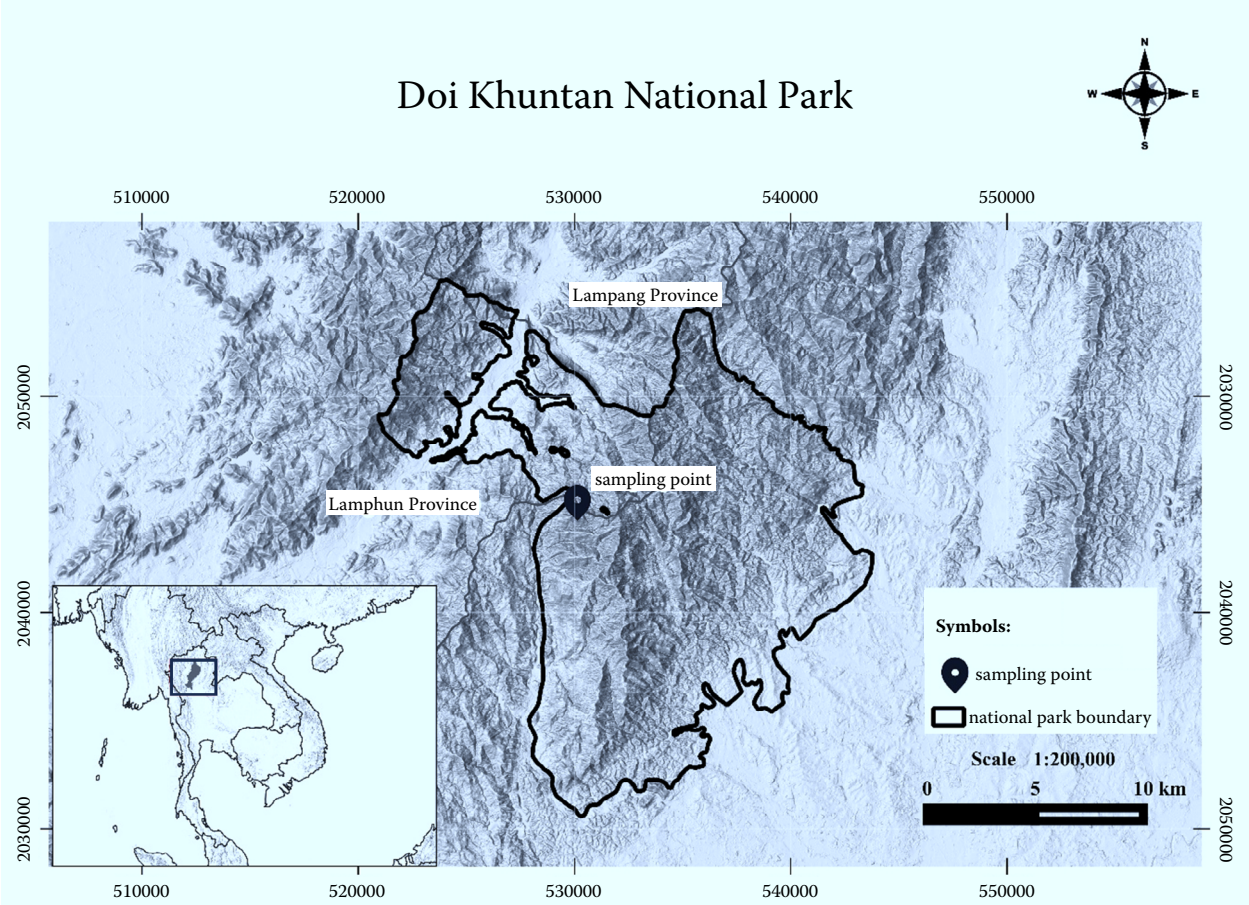

Figure 1. Location map of Doi Khuntan National Park, Lamphun Province, northern Thailand black circle – the study site; black line – national park boundary; the inset map shows the regional context in mainland Southeast Asia

surface fires. Palakit and Pumijumnong (2024) reported that the diameter at breath height of *P. Kesiya* at this site reaches up to 72.2 cm, and that its seedlings and saplings are generally distributed throughout the area, indicating active natural regeneration.

Tree-ring data collection and chronology development. In 2018, fifty-two increment cores were extracted from selected 26 dominant and healthy *P. kesiya* trees with straight boles and no visible damage or disease using a 40-cm long, 0.5-cm diameter increment borer (Haglöf Sweden AB, Sweden). Two cores were extracted at breast height (1.3 m) from opposite sides of each tree to minimise non-climatic influences. Cores were air-dried, mounted on wooden supports, and progressively sanded with 200–600 grit abrasive paper until ring boundaries were clearly visible under a stereomicroscope.

Ring widths were measured to the nearest measurement resolution 0.001 mm using a TA Unislide Tree Ring Measurement System (Velmex Inc., USA) interfaced with MeasureJ2X software (Version 3.2.1, 2002). Cross-dated was performed using standard visual and statistical techniques verified with COFECHA software (Holmes 1983). The cross-dated series were standardised using ARSTAN software (Cook, Krusic 2005) to remove age-related growth trends while preserving climate signals. Individual series were detrended using negative exponential curves for younger trees with strong biological trends or straight lines with negative/zero slope for older trees, followed by standardisation using a 66-year cubic smoothing spline (50% frequency-response cutoff). Three chronology versions were generated: standard (*STD*: low-frequency variance retained), residual (*RES*: pre-whitened to remove autocorrelation), and arstan (*ARS*: a compromise between *STD* and *RES*). Chronology quality was assessed using expressed population signal (*EPS*), mean inter-series correlation (*Rbar*), and signal-to-noise ratio (*SNR*) with *EPS* ≥ 0.85 considered reliable for dendroclimatic studies (Wigley et al. 1984).

https://doi.org/10.17221/78/2025-JFS

False ring analysis. False rings were visually identified based on anatomical criteria, including abrupt changes in tracheid cell wall thickness and colour differences within an annual ring. Annual false ring frequency (*F*) was calculated as the proportion of cores containing false rings relative to the total number of cores observed each year, see Equation (1) below:

$$F = \frac{N}{n} \quad (1)$$

where:

F – annual false ring frequency;

N – number of cores with false rings;

n – the total number of samples observed.

To correct for variations in sample depth over time, stabilised false ring frequency (*f*) was calculated as $f = Fn^{0.5}$ following Battipaglia et al. (2014). This stabilised index served as the dependent variable in climate response analyses.

Climate data and response analysis. Instrumental climate data (1951–2018) were obtained from the Lampang Meteorological Station (Station ID: 48303, 18.27°N, 99.52°E, elevation: 242 m a.s.l.), located approximately 45 km northeast of the sampling site. Variables included monthly rainfall, mean/maximum/minimum temperatures, extreme temperatures, and relative humidity. Regional climate indices – equatorial southern oscillation index (*EQ_SOI*) and equatorial sea surface temperature (*EQ_SST*) – were obtained from NOAA's Physical Sciences Laboratory website (https://psl.noaa.gov/). Seasonal variables were defined based on the Walter climate diagram for Lampang, with wet periods (April–October) and dry periods (November–March).

Correlation analyses identified relationships between tree-ring indices (*RES* chronology, false-ring index) and monthly/seasonal/annual climate variables. Multiple linear regression with stepwise selection ($P < 0.05$ entry/exit) identified key growth drivers. Climate variables showing strongest correlation were selected for reconstruction using simple linear regression models. Reconstruction skill was evaluated using the Pearson correlation coefficient (*Rp*), sign-product test (*ST*), reduction of error (*RE*), *t*-value, mean, and standard deviation (*SD*) statistics during calibration and verification periods. For April–July mean temperature and relative humidity reconstructions based on the *RES* index, 1996–2018 served as calibration and 1951–1995 as verification. For March maximum temperature and April extreme minimum temperature reconstructions based on false-ring index, 1951–1984 was calibration and 1985–2018 verification. Trend significance in reconstructed series was assessed using Mann-Kendall tests.

RESULTS

Chronology characteristics and quality. The 48 successfully cross-dated cores (from 26 trees) produced an 83-year chronology spanning 1936–2018 (Figure 2). Sample depth exceeded 20 cores for most of the period, ensuring adequate replication. Descriptive statistics for the three chronology versions are presented in Table 1. The Residual (*RES*) chronology, selected for all climate analyses, exhibited optimal characteristics with mean sensitivity of 0.171, first-order autocorrelation of –0.088, mean inter-series correlation of 0.228, *SNR* of 6.85, and *EPS* consistently above the 0.85 reliability threshold throughout the common period.

Climate-growth relationships. Correlation analysis revealed strong moisture control on *P. kesiya* radial growth [Table S1 in the Electronic Supplementary Material (ESM)]. The most significant positive correlations occurred with March precipitation ($r = 0.39$, $P < 0.01$) and April–July relative humidity ($r = 0.48$, $P < 0.01$). Growth also showed positive responses to previous year's July rainfall ($r = 0.26$, $P < 0.05$) and dry-season humidity ($r = 0.33$, $P < 0.01$), indicating carryover effects. In contrast, consistently negative and highly significant correlations were found with wet-season temperatures, particularly April–July mean temperature ($r = –0.47$, $P < 0.01$), April mean temperature ($r = –0.42$), and June extreme maximum temperature ($r = –0.42$). Regional climate indices showed significant teleconnections: positive correlations with *EQ_SOI* during current January ($r = 0.33$) and previous November ($r = 0.33$), and negative correlations with *EQ_SST* in previous August–December ($r = –0.25$ to $–0.32$), indicating La Niña-like conditions promote growth.

Multiple regression analysis identified four key growth predictors explained 40.6% of variance: March rainfall (RF_{Mar}), April–July mean temperature ($MT_{Apr–Jul}$), September relative humidity (RH_{Sept}), and November extreme minimum temperature (EMT_{Nov}).

https://doi.org/10.17221/78/2025-JFS

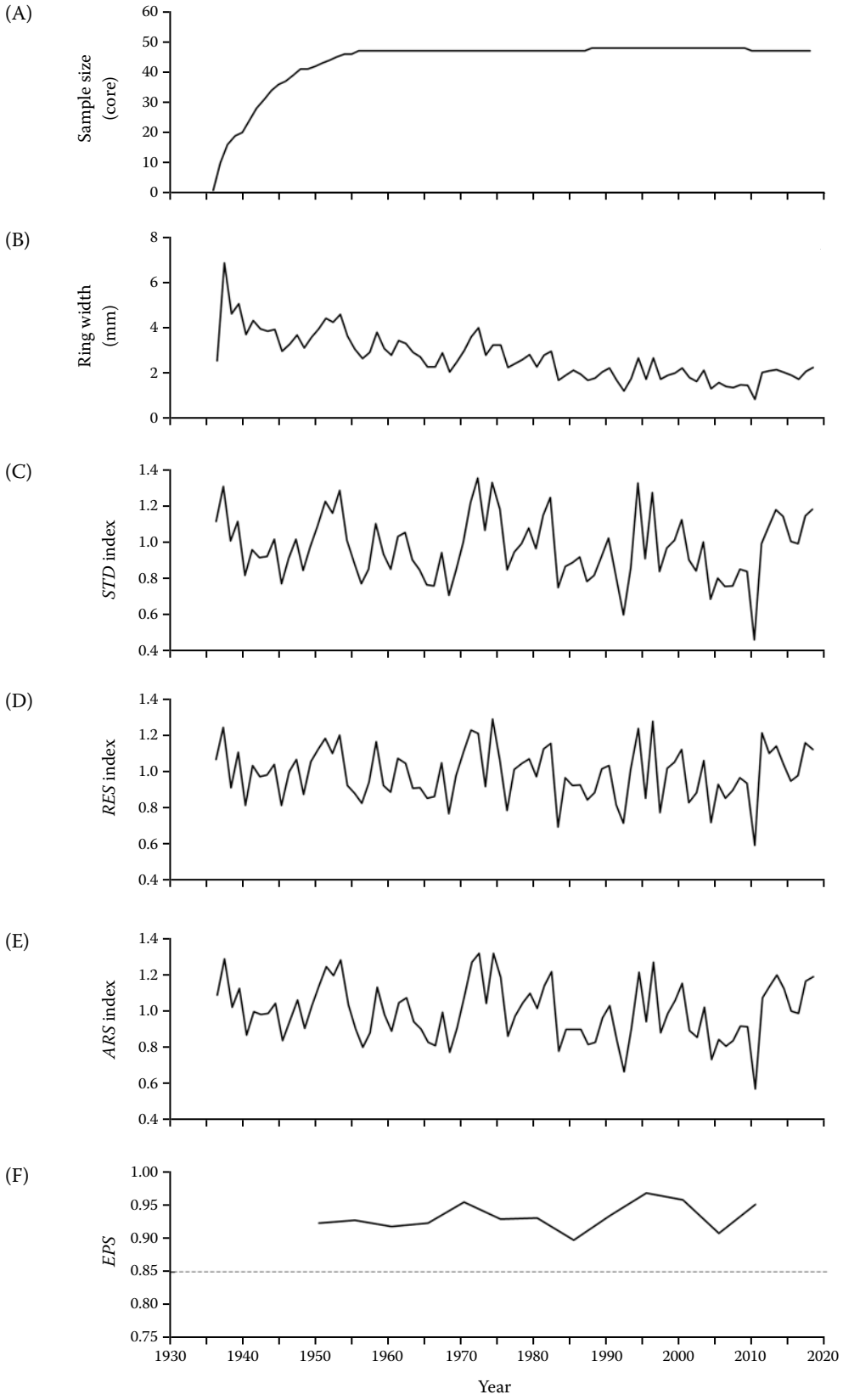

Figure 2. Chronology characteristics of *Pinus kesiya* from Doi Khuntan National Park: (A) sample depth, (B) mean annual ring width (mm), (C) *STD* (standard) chronology, (D) *RES* (residual) chronology, (E) *ARS* (arstan) chronology, (F) expressed population signal (*EPS*)

https://doi.org/10.17221/78/2025-JFS

Table 1. Descriptive statistics for standard (*STD*), residual (*RES*), and arstan (*ARS*) chronologies of *Pinus kesiya* from Doi Khuntan National Park (1936–2018, n = 48 cores)

Statistic	*STD*	*RES*	*ARS*
Mean index	0.973	0.992	0.990
Standard deviation	0.174	0.145	0.155
Mean sensitivity	0.165	0.171	0.144
Autocorrelation (order 1)	0.365	–0.088	0.368
Mean inter-series correlation	0.208	0.228	0.208
Signal-to-noise ratio	5.123	6.850	5.123
Expressed population signal	0.923	0.932	0.923

The climate-growth relationship can be mathematically expressed as shown in Equation (2):

$$R = 1.232 + 0.001\ RF_{Mar} - 0.081\ MT_{Apr–Jul} + \\ + 0.22\ RH_{Sept} + 0.01\ EMT_{Nov} \quad (2)$$

where:
RF_{Mar} – March rainfall;
$MT_{Apr–Jul}$ – April–July mean temperature;
RH_{Sept} – September relative humidity;
EMT_{Nov} – November extreme minimum temperature.

False-ring climate drivers. False rings occurred in 42% of years, with peak frequencies in 1953, 1977, and 1993 (Figure 3). Correlation analysis revealed false-ring formation was associated with specific intra-annual conditions: negative correlations with April–July rainfall (r = –0.35, P < 0.01) and July relative humidity (r = –0.45, P < 0.01), and with March maximum temperature (r = –0.48, P < 0.01) and April extreme minimum temperature (r = –0.49, P < 0.01). This pattern suggests false rings form during cool-dry spells in the dry-to-wet season transition rather than hot droughts. The negative correlation with May *EQ_SOI* (r = –0.35) further links false-ring formation to El Niño-like conditions, which typically delay monsoon onset in the region (Table S2 in the ESM).

Multiple regression identified seven significant predictors of false-ring frequency (F): January rainfall (RF_{Jan}), March mean maximum temperature ($MMaT_{Mar}$), April extreme minimum temperature (EMT_{Apr}), May *EQ_SOI* (EQ_SOI_{May}), June rainfall (RF_{Jun}), July relative humidity (RH_{Jul}), and October rainfall (RF_{Oct}), collectively explaining 65.6% of variance (R^2 = 0.656, P < 0.001) as summarised by the model Equation (3). The negative coefficients for temperature variables (–0.240 for $MMaT_{Mar}$, –0.142 for EMT_{Apr}) confirmed the cool-temperature association, while negative coefficients for mid-wet season moisture variables indicated drought stress involvement.

$$F = 21.067 + 0.012\ RF_{Jan} + \\ - 0.240\ MMaT_{Mar} - 0.142\ EMT_{Apr} + \\ - 0.193\ EQ\_SOI_{May} - 0.002\ RF_{Jun} + \\ - 0.101\ RH_{Jul} - 0.003\ RF_{Oct} \quad (3)$$

where:
F – false-ring frequency;
RF_{Jan} – January rainfall;
$MMaT_{Mar}$ – March mean maximum temperature;
EMT_{Apr} – April extreme minimum temperature;
EQ_SOI_{May} – May *EQ_SOI* (equatorial southern oscillation index);
RF_{Jun} – June rainfall;
RH_{Jul} – July relative humidity;
RF_{Oct} – October rainfall.

Climate reconstruction and trend. Four climate variables were reconstructed based on strong tree-ring correlations: April–July mean temperature ($MT_{Apr–Jul}$) and relative humidity ($RH_{Apr–Jul}$) from the *RES* chronology, and March mean maximum temperature in ($MMaT_{Mar}$) and April extreme minimum temperature (EMT_{Apr}) from the false-ring index. Calibration statistics were significant for all models (Tables 2 and 3), with verification statistics confirming model reliability. Reconstruction Equations (4–7) are:

$$MT_{Apr–Jul} = 3.9068 - 0.1(RES) \quad (4)$$

$$RH_{Apr–Jul} = 0.0278(RES) - 1.0107 \quad (5)$$

$$MMaT_{Mar} = 37.059 - 0.8382(F) \quad (6)$$

$$EMT_{Apr} = 20.392 - 1.2372(F) \quad (7)$$

https://doi.org/10.17221/78/2025-JFS

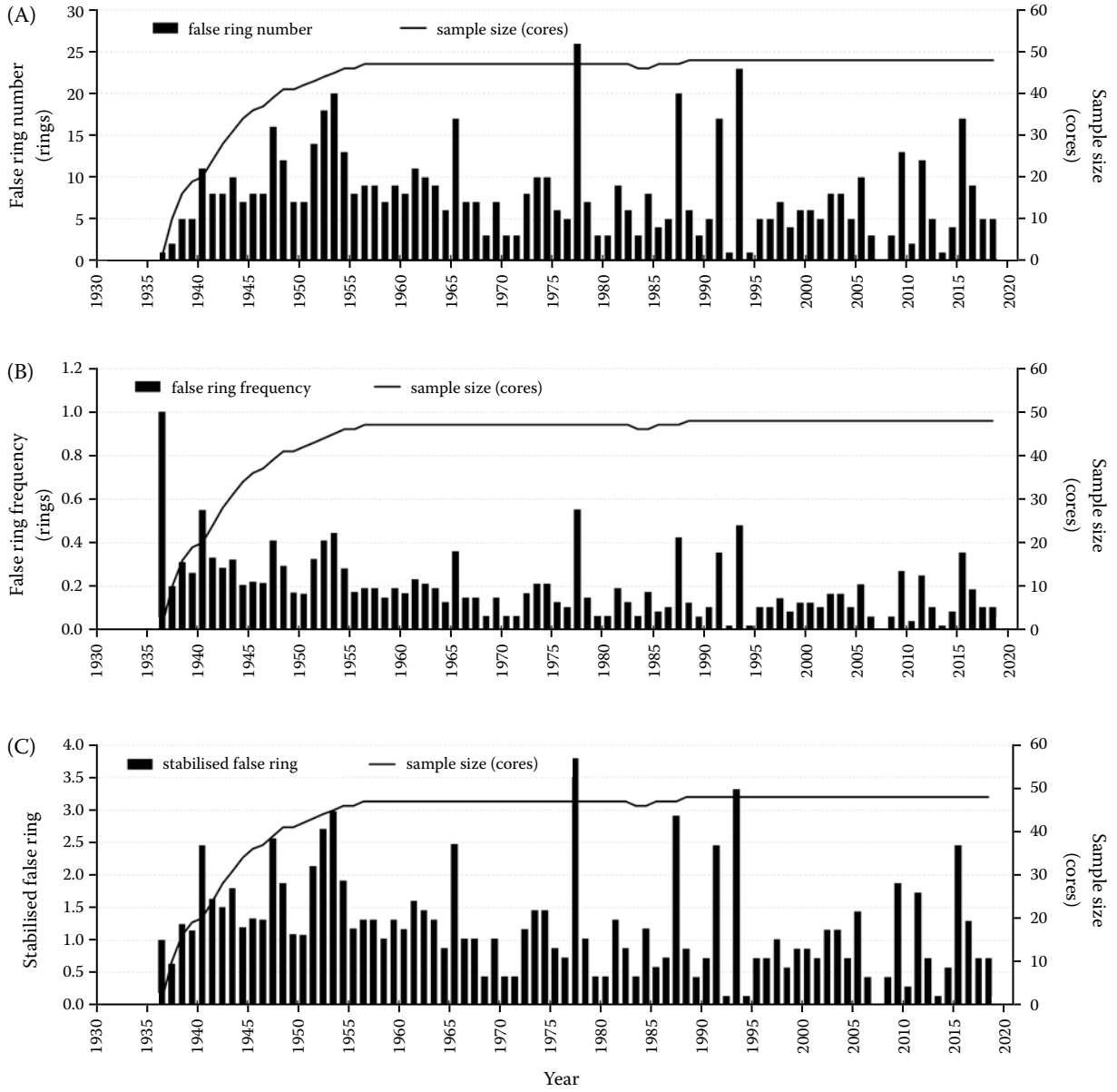

Figure 3. False ring occurrences in *Pinus kesiya* at Doi Khuntan National Park: (A) annual count of false rings (number of cores with a false ring), (B) raw false ring frequency (proportion of cores with a false ring each year), and (C) stabilised false ring index adjusted for variations in sample depth

Table 2. Calibration and verification statistics for climate reconstruction from the *RES* chronology

Statistic	$MT_{Apr–Jul}$		$RH_{Apr–Jul}$	
	calibration[1]	verification[2]	calibration[1]	verification[2]
Pearson correlation	0.5024*	0.4467*	0.6014*	0.3591*
Sign product test	7*	17	9	19
Reduction of error (*RE*)	0.2524*	0.1528*	0.3617*	0.0530
T-test	1.7809*	1.8299*	2.2260*	1.9962*
Degree of freedom	21	43	21	43

*Significance at $P < 0.05$; [1]calibration period: 1996–2018; [2]verification period: 1951–1995; *RES* – residual chronology; $MT_{Apr–Jul}$ – April–July mean temperature; $RH_{Apr–Jul}$ – April–July relative humidity

https://doi.org/10.17221/78/2025-JFS

Table 3. Calibration and verification statistics for climate reconstruction from the false-ring index

Statistic	$MMaT_{Mar}$		EMT_{Apr}	
	calibration[1]	verification[2]	calibration[1]	verification[2]
Pearson correlation	0.5774*	0.3925*	0.5588*	0.3407*
Sign product test	8*	10*	8*	6*
Reduction of error (*RE*)	0.3333*	0.2248*	0.3125*	0.2358*
T-test	1.5705*	1.8488*	2.3354*	0.3929*
Degree of freedom	32	32	32	32

*Significance at $P < 0.05$; [1]calibration period: 1951–1984; [2]verification period: 1985–2018; $MMaT_{Mar}$ – March mean maximum temperature; EMT_{Apr} – April extreme minimum temperature

The reconstructed series revealed climate trends over the 83-year period (Figures 4–7). $MT_{Apr–Jul}$ increased by +0.10 °C (+0.012 °C/decade), although this trend was not statistically significant (Mann-Kendall $S = 106$, $Z = 0.41$, $P = 0.68$). $RH_{Apr–Jul}$ declined by –0.51% (–0.061%/decade), but similarly lacked statistical significance (Mann-Kendall $S = -106$, $Z = 0.41$, $P = 0.68$). In contrast, statistically significant warming was detected for the remaining variables. Most pronounced warming occurred in $MMaT_{Mar}$, which increased by +0.67 °C (+0.081 °C/decade, Mann-Kendall $S = 1040$, $Z = 4.09$, $P < 0.01$). EMT_{Apr} showed similar warming of +0.98 °C (+0.119 °C/decade, Mann-Kendall $S = 1040$, $Z = 4.09$, $P < 0.01$).

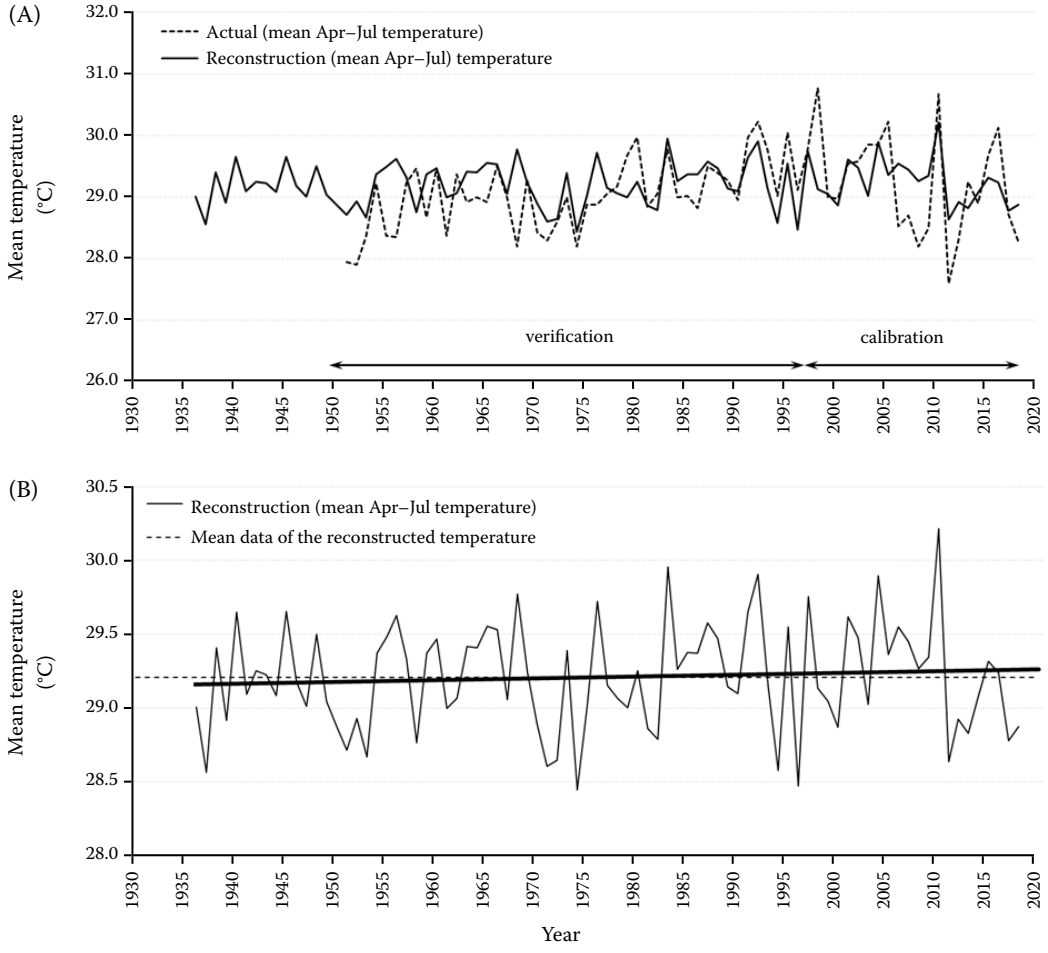

Figure 4. Reconstruction of the April–July mean temperature ($MT_{Apr–Jul}$): (A) actual and reconstructed $MT_{Apr–Jul}$ series, (B) the full reconstructed $MT_{Apr–Jul}$ series from 1936–2018 including its long-term trend

https://doi.org/10.17221/78/2025-JFS

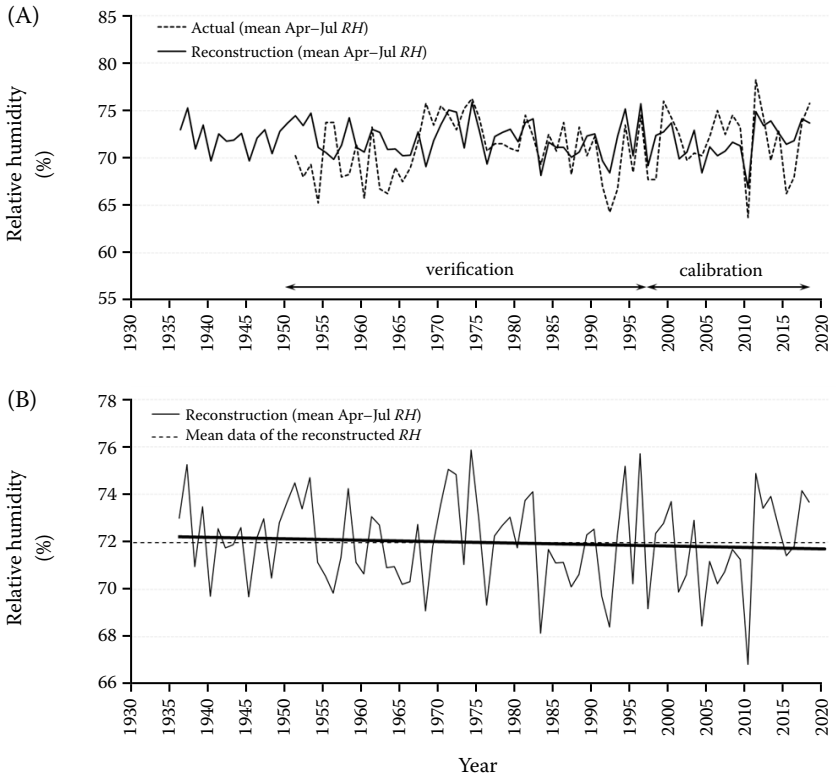

Figure 5. Reconstruction of the April–July relative humidity ($RH_{Apr–Jul}$): (A) actual and reconstructed $RH_{Apr–Jul}$, (B) the full reconstructed $RH_{Apr–Jul}$ series from 1936–2018 including its long-term trend

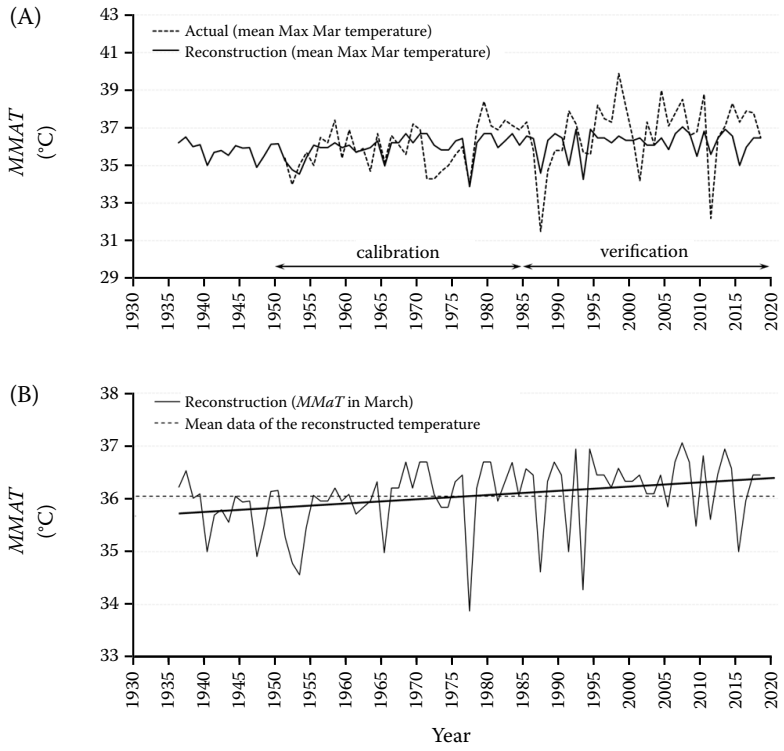

Figure 6. Reconstruction of the mean maximum temperature in March ($MMaT_{Mar}$): (A) actual and reconstructed $MMaT_{Mar}$, (B) the full reconstructed $MMaT_{Mar}$ series from 1936–2018 including its long-term trend

https://doi.org/10.17221/78/2025-JFS

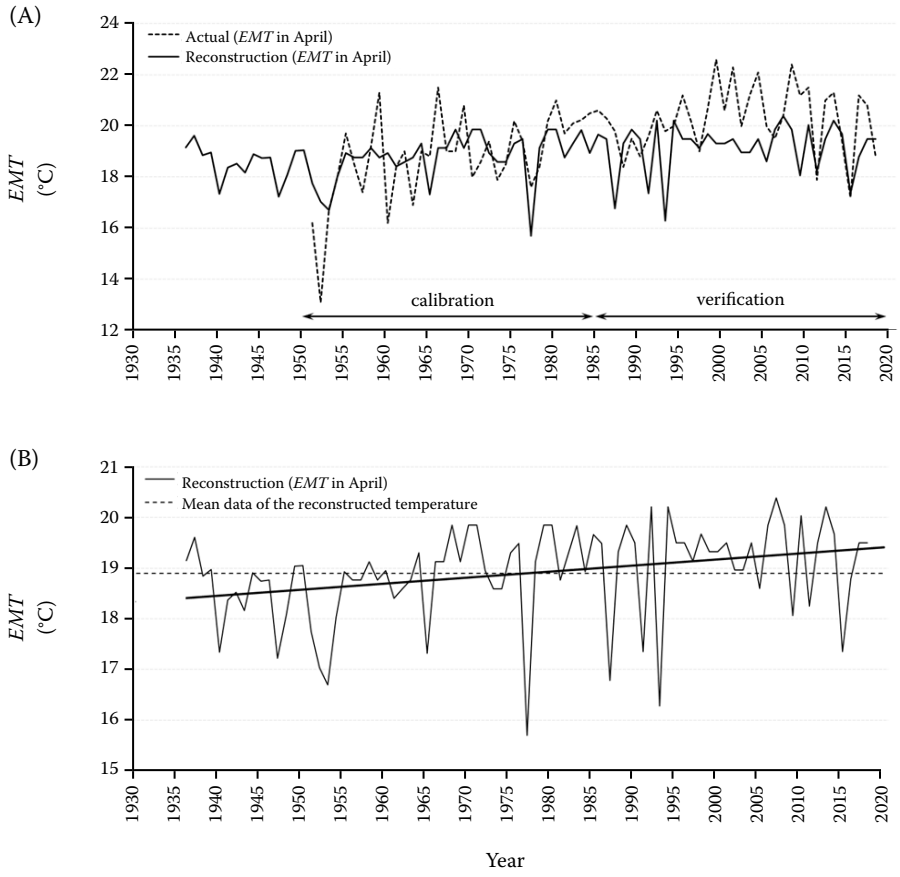

Figure 7. Reconstruction of the extreme minimum temperature in April (EMT_{Apr}): (A) actual and reconstructed EMT_{Apr}, (B) the full reconstructed EMT_{Apr} series from 1936–2018 including its long-term trend

DISCUSSION

Growth-climate relationships and physiological mechanisms. Comparative analysis showed the sensitivity of *P. Kesiya* is moderate relative to other regional species– higher than managed *P. kesiya* plantations but lower than teak (*Tectona grandis*) and comparable to Tenasserim pine (*P. latteri*) (Pumijumnong, Eckstein 2011).The strong positive response of *P. kesiya* to March precipitation confirms the critical importance of pre-monsoon moisture in breaking cambial dormancy after the dry season. This rainfall likely rehydrates tissues and enables carbohydrate mobilisation for initial earlywood formation, consistent with findings for other tropical pines (Pumijumnong, Eckstein 2011; Rathgeber et al. 2016). The equally strong influence of April–July relative humidity, often showing stronger correlations than precipitation itself, emphasises the role of atmospheric moisture in maintaining favourable plant water status through reduced vapor pressure deficit (Bauman et al. 2022), thereby supporting sustained cambial activity and photosynthetic carbon gain (Grossiord et al. 2020).

The consistent negative correlation with wet-season temperature reveals important thermal constraints on growth processes. Higher temperatures increase atmospheric evaporative demand, potentially forcing stomatal closure and reducing photosynthetic efficiency even when soil moisture appears adequate – a phenomenon known as 'atmospheric drought' (Kannenberg et al. 2020). This demonstrates the crucial interaction between temperature and moisture in determining growth rates, as warmer conditions during the wet season can effectively negate the benefits of rainfall by increasing plant water stress. Similar temperature-mediated drought effects have been observed in Khasi pine populations in Northeast India (Thomte et al. 2022b).

The influence of large-scale climate patterns, particularly the positive correlation with *EQ_SOI* (La Niña conditions), provides important context for these local responses. La Niña events create

https://doi.org/10.17221/78/2025-JFS

favourable growth conditions through enhanced cloud cover, reduced temperatures, and increased rainfall availability in mainland Southeast Asia (Boisvenue, Running 2006). This teleconnection pattern illustrates how global climate dynamics directly influence local forest productivity, with La Niña conditions mitigating the atmospheric drought stress that would otherwise limit carbon assimilation during critical growth periods.

False rings as intra-annual climate proxies. Our analysis advances the understanding of false-ring formation in tropical pines by demonstrating their association with specific cool-dry conditions during seasonal transitions rather than simple drought stress. The negative correlations with March–April temperatures contradict the conventional expectation that false rings form during hot droughts, instead suggesting they develop when a period of cooler, drier conditions interrupts the early wet-season growth phase. This aligns with the physiological mechanism where temporary drought stress causes cambial activity to cease, forming a false latewood-like band, followed by resumption of growth under renewed favourable conditions (De Micco et al. 2016; Therrell et al. 2020).

This refined understanding has important implications for paleoclimatology. False rings in *P. kesiya* appear to specifically mark years with irregular monsoon onset characterised by false starts – initial pre-monsoon rains followed by a return to dry conditions – rather than years with uniformly deficient rainfall. The link to El Niño-like conditions (negative *EQ_SOI*) supports this interpretation, as such phases are associated with delayed or weaker monsoon onset in the region. Similar patterns have been reported for teak (*T. grandis*) in Thailand, where false rings form in response to pre-monsoon drought followed by monsoon onset (Palakit et al. 2012).

Multi-proxy climate reconstruction and trends. The integrated use of ring-width and false-ring indices represents a significant advancement in tropical dendroclimatology, providing complementary information at different temporal scales. While traditional ring-width chronologies effectively capture growing-season conditions (April–July), the false-ring indices provide unique insight into transitional periods (March–April), particularly regarding temperature extremes and moisture stress. This multi-proxy approach addresses a key challenge in tropical dendroecology where conventional annual measurements may miss sub-seasonal climate signals (Pumijumnong, Palakit 2020).

The reconstructed climate trends reveal a clear pattern of warming and drying in the Doi Khuntan highlands over the past century, consistent with regional climate change observations (Tammadid et al. 2023). The most pronounced warming in April extreme minimum temperatures (+0.98 °C over 83 years) is particularly ecologically significant, as nighttime warming can affect respiratory processes, frost-sensitive phenology, and water balance differently than daytime warming. The concurrent decline in early wet-season humidity and increasing false-ring frequency suggest enhanced atmospheric drought stress, potentially explaining observed growth reductions in recent decades despite adequate precipitation in some years.

These trends align with broader regional patterns identified in paleoclimate studies. Payomrat et al. (2018) documented similar warming in northwestern Thailand since 1788 using stable carbon isotopes, while Pumijumnong et al. (2020) identified historical drought patterns in teak oxygen isotope records that correspond to our observed humidity decline. The consistency across multiple proxies and species strengthens the conclusion that northern Thailand is experiencing a pronounced shift toward warmer and drier conditions, with important implications for montane forest ecosystems.

Implications for forest management. The demonstrated sensitivity of *P. kesiya* to pre-monsoon moisture and wet-season temperature implies that projected changes in monsoon timing and intensity may substantially affect forest productivity and resilience. Climate models project increased rainfall variability and more frequent dry spells during the wet season for mainland Southeast Asia (IPCC 2022), conditions likely to increase false-ring formation and reduce radial growth. The increasing frequency of false rings itself serves as a biological indicator of more frequent sub-seasonal drought events, which may ultimately affect forest structure, species composition, and ecosystem services, including carbon sequestration and watershed protection.

Management strategies should focus on enhancing forest resilience through water conservation measures, protection of catchment areas, and potentially assisted migration of drought-adapted provenances where appropriate (Aitken et al. 2008).

https://doi.org/10.17221/78/2025-JFS

The use of tree-ring data can help identify particularly vulnerable stands and prioritise management interventions (D'Orangeville et al. 2018). Integrating these dendroecological insights with adaptive forest management will be crucial for maintaining pine forest ecosystems and their associated services under changing climate conditions (Seidl et al. 2016).

Limitations and future research directions. While this study provides valuable insights, several limitations should be acknowledged. First, the 83-year chronology, while robust for the site, limits analysis of long-term (centennial-scale) climate variability and places the reconstruction largely within the period of anthropogenic warming. Second, potential 'divergence' between tree growth and climate trends in recent decades, observed in some temperate forests, could not be fully assessed but should be monitored. Third, the influence of juvenile growth trends in the earliest chronology segment (pre-1950) may affect early reconstruction accuracy, though our detrending methods minimize this effect. Finally, as a single-site reconstruction, its regional representativeness should be validated through additional sampling.

Future research should expand spatial coverage across the species' range to capture regional gradients, incorporate additional climate data sources (e.g. reanalysis products), and utilise stable isotope analysis ($\delta^{18}O$, $\delta^{13}C$) in tree rings to further validate reconstructions and provide physiological context (Payomrat et al. 2018; Kharmawlong et al. 2023). Combining these approaches will enhance our understanding of climate impacts on tropical montane forests and improve predictive capacity for future changes.

CONCLUSION

This study establishes *P. kesiya* as a sensitive climate proxy in northern Thailand's montane forests and demonstrates the value of multi-proxy dendroclimatological approaches. Radial growth of *P. kesiya* is strongly controlled by pre-monsoon (March) moisture availability and wet-season (April–July) temperature and humidity conditions, with significant negative responses to warmer wet seasons indicating temperature-mediated drought stress. False rings serve as valuable intra-annual climate proxies, forming specifically during cool-dry spells in the dry-to-wet season transition rather than during hot droughts, and are associated with El Niño-like conditions that delay monsoon onset. Multi-proxy climate reconstructions reveal significant warming since the 1930s, most pronounced in April extreme minimum temperature (+0.98 °C over 83 years), alongside declining wet-season humidity, indicating increasing atmospheric drought stress. The integrated ring-width and false-ring approach provides enhanced temporal resolution for tropical dendroclimatology, capturing both seasonal and sub-seasonal climate signals. These findings provide a critical high-resolution baseline for assessing climate change impacts on montane pine forests and inform the development of adaptive management strategies to enhance ecosystem resilience under changing climatic conditions in mainland Southeast Asia.

Acknowledgement: We thank the chief and staff of Doi Khuntan National Park for their support and assistance with fieldwork. The necessary permits for tree-core sampling were obtained from the Department of National Parks, Wildlife and Plant Conservation (No. 0907.4/8748). We also thank the Laboratory of Tropical Dendrochronology (LTD), Faculty of Forestry, Kasetsart University, for providing facilities and equipment.

REFERENCES

Aitken S.N., Yeaman S., Holliday J.A., Wang T., Curtis-McLane S. (2008): Adaptation, migration or extirpation: Climate change outcomes for tree populations. Evolutionary Applications, 1: 95–111.

Battipaglia G., De Micco V., Brand W.A., Saurer M., Aronne G., Linke P., Cherubini P. (2014): Drought impact on water use efficiency and intra-annual density fluctuations in *Erica arborea* on Elba (Italy). Plant, Cell and Environment, 37: 382–391.

Bauman D., Fortunel C., Delhaye G., Malhi Y., Cernusak L., Bentley L., Rifai S., Aguirre-Gutiérrez J., Oliveras I., Phillips O., Mcnellis B., Bradford M., Laurance S., Hutchinson M.F., Dempsey R., Santos-Andrade P.E., Ninantay-Rivera H.R., Paucar J., McMahon S. (2022): Tropical tree mortality has increased with rising atmospheric water stress. Nature, 608: 1–6.

Boisvenue C., Running S.W. (2006): Impacts of climate change on natural forest productivity – Evidence since the middle of the 20th century. Global Change Biology, 12: 862–882.

https://doi.org/10.17221/78/2025-JFS

Cook E.R., Krusic P. (2005): Program ARSTAN: A tree-ring standardization program based on detrending and autoregressive time series modeling, with interactive graphics. Available at: https://sheppard.ltrr.arizona.edu/presession/arsreadme_135.doc (accessed Sept 14, 2025)

D'Orangeville L., Houle D., Duchesne L., Phillips R.P., Bergeron Y., Kneeshaw D. (2018): Beneficial effects of climate warming on boreal tree growth may be transitory. Nature Communications, 9: 3213.

De Micco V., Balzano A., Čufar K., Aronne G., Gričar J., Merela M., Battipaglia G. (2016): Timing of false ring formation in *Pinus halepensis* and *Arbutus unedo* in southern Italy: Outlook from an analysis of xylogenesis and tree-ring chronologies. Frontiers in Plant Science, 7: 1–14.

Feeley K.J., Rehm E.M., Machovina B. (2012): Perspective: The responses of tropical forest species to global climate change: Acclimate, adapt, migrate, or go extinct? Frontiers in Biogeography, 4: 69–82.

Grossiord C., Buckley T.N., Cernusak L.A., Novick K.A., Poulter B., Siegwolf R.T.W., Sperry J.S., McDowell N.G. (2020): Plant responses to rising vapor pressure deficit. New Phytologist, 226: 1550–1566.

Herrera-Ramirez D., Andreu-Hayles L., Del Valle J.I., Santos G.M., Gonzalez P.L.M. (2017): Nonannual tree rings in a climate-sensitive *Prioria copaifera* chronology in the Atrato River, Colombia. Ecology and Evolution, 7: 6334–6345.

Hofer M., Horak J. (2020): Extending limited in situ mountain weather observations to the baseline climate: A true verification case study. Atmosphere, 11: 1256.

Holmes R.L. (1983): Computer-assisted quality control in tree-ring dating and measurement. Tree-Ring Bulletin, 43: 69–78.

IPCC (2022): Climate Change 2022: Impacts, Adaptation and Vulnerability. Contribution of Working Group II to the Sixth Assessment Report of the Intergovernmental Panel on Climate Change. Cambridge, Cambridge University Press: 3056.

Kannenberg S.A., Schwalm C.R., Anderegg W.R.L. (2020): Ghosts of the past: How drought legacy effects shape forest functioning and carbon cycling. Ecology Letters, 23: 891–901.

Khamyong S., Anongrak N. (2016): Carbon and nutrient storages in an upper montane forest at Mt. Inthanon summit, northern Thailand. Environment and Natural Resources Journal, 14: 26–38.

Kharmawlong R., Upadhyay K.K., Tripathi S.K. (2023): Detecting the legacies of climatic extremes through radial growth releases in *Pinus kesiya* Royle ex Gordon in Shillong, Meghalaya, Northeast India. Environment and Ecology, 41: 2766–2774.

Linasmita V., Pumijumnong N. (2004): Seasonal variation on cambial activity of *Pinus kesiya* in Doi Khuntan national park, Lampang Province. Environment and Natural Resources Journal, 2: 1–10.

Marod D., Thinkampheang S., Phumphuang W., Yarnvudhi A., Thongsawi J., Kachina P., Nakashizuka T., Kurokawa H., Hermhuk S. (2025): Relationship between climate changes and forest dynamics along altitudinal gradients at Doi Suthep-Pui national park, northern Thailand. Forests, 16: 114.

Palakit K., Pumijumnong N. (2024): Impact of increment coring on growth and mortality across various size classes of Khasi pine (*Pinus kesiya*) in northern Thailand. Forests, 15: 1444.

Palakit K., Siripattanadilok S., Duangsathaporn K. (2012): False ring occurrences and their identification in teak (*Tectona grandis*) in north-eastern Thailand. Journal of Tropical Forest Science, 24: 387–398.

Palakit K., Duangsathaporn K., Siripatanadilok S. (2015): Climatic fluctuations trigger false ring occurrence and radial-growth variation in teak (*Tectona grandis* L.f.). iForest – Biogeosciences and Forestry, 9: 286–293.

Payomrat P., Liu Y., Pumijumnong N., Li Q., Song H. (2018): Tree-ring stable carbon isotope-based June–September maximum temperature reconstruction since AD 1788, north-west Thailand. Tellus Series B: Chemical and Physical Meteorology, 70: 1443655.

Pumijumnong N., Eckstein D. (2011): Reconstruction of premonsoon weather conditions in northwest Thailand from the tree-ring widths of *Pinus merkusii* and *Pinus kesiya*. Trees, 25: 125–132.

Pumijumnong N., Palakit K. (2020): Effects of climate variability on the annual and intra-annual ring formation of *Pinus merkusii* growing in central Thailand. Environment and Natural Resources Journal, 18: 234–248.

Pumijumnong N., Bräuning A., Sano M., Nakatsuka T., Muangsong C., Buajan S. (2020): A 338-year tree-ring oxygen isotope record from Thai teak captures the variations in the Asian summer monsoon system. Scientific Reports, 10: 8966.

Rakthai S., Fu P.L., Fan Z.X., Gaire N.P., Pumijumnong N., Eiadthong W., Tangmitcharoen S. (2020): Increased drought sensitivity results in a declining tree growth of *Pinus latteri* in northeastern Thailand. Forests, 11: 361.

Rathgeber C.B.K., Cuny H.E., Fonti P. (2016): Biological basis of tree-ring formation: A crash course. Frontiers in Plant Science, 7: 734.

Seidl R., Spies T.A., Peterson D.L., Stephens S.L., Hicke J.A. (2016): Searching for resilience: Addressing the impacts of changing disturbance regimes on forest ecosystem services. Journal of Applied Ecology, 53: 120–129.

https://doi.org/10.17221/78/2025-JFS

Seidl R., Thom D., Kautz M., Martin-Benito D., Peltoniemi M., Vacchiano G., Wild J., Ascoli D., Petr M., Honkaniemi J., Lexer M.J., Trotsiuk V., Mairota P., Svoboda M., Fabrika M., Nagel T.A., Reyer C.P.O. (2017): Forest disturbances under climate change. Nature Climate Change, 7: 395–402.

Singh M., Griaud C., Collins C.M. (2021): An evaluation of the effectiveness of protected areas in Thailand. Ecological Indicators, 125: 107536.

Speer J.H. (2010): Fundamentals of Tree-Ring Research. Tucson, University of Arizona Press: 333.

Strachan S., Kelsey E.P., Brown R.F., Dascalu S., Harris F., Kent G., Lyles B., McCurdy G., Slater D., Smith K. (2016): Filling the data gaps in mountain climate observatories through advanced technology, refined instrument siting, and a focus on gradients. Mountain Research and Development, 36: 518–527.

Tammadid W., Nantasom K., Sirksiri W., Vanitchung S., Promjittiphong C., Limsakul A., Hanpattanakit P. (2023): Future projections of precipitation and temperature in northeast, Thailand using bias-corrected global climate models. Chiang Mai Journal of Science, 50: 1–8.

Temchai T., Saengswang M., Jaikaew P., Deekaew P., Thammalangka P., Hengswang D., Wanmanee S., Jitra N., Thongsuk P., Thongkerd T. (2018): The relative between phenology and climates factor of plants in pine-dry dipterocarp forest, Suphanburi province, Thailand. Journal of Thailand National Parks Research, 2: 122–136.

Thammanu S., Han H., Marod D., Zang L., Jung Y., Soe K.T., Onprom S., Chung J. (2020): Non-timber forest product utilization under community forest management in northern Thailand. Forest Science and Technology, 17: 1–15.

Thammanu S., Han H., Ekanayake E.M.B.P., Jung Y., Chung J. (2021a): The impact on ecosystem services and the satisfaction therewith of community forest management in northern Thailand. Sustainability, 13: 13474.

Thammanu S., Han H., Marod D., Srichaichana J., Chung J. (2021b): Above-ground carbon stock and REDD+ opportunities of community-managed forests in northern Thailand. PLoS ONE, 16: e0256005.

Therrell M.D., Elliott E.A., Meko M.D., Bregy J.C., Tucker C.S., Harley G.L., Maxwell J.T., Tootle G.A. (2020): Streamflow variability indicated by false rings in Bald Cypress [*Taxodium distichum* (L.) Rich.]. Forests, 11: 1100.

Thomte L., Bhagabati A.K., Shah S.K. (2022b): Soil moisture-based winter-spring drought variability over West Karbi Anglong region, Assam, Northeast India using tree-rings of *Pinus kesiya*. Environmental Challenges, 7:100512.

Thomte L., Shah S.K., Mehrotra N., Bhagabati A.K., Saikia A. (2022a): Influence of climate on multiple tree-ring parameters of *Pinus kesiya* from Manipur, Northeast India. Dendrochronologia, 71: 125906.

Thomte L., Shah S.K., Mehrotra N., Saikia A., Bhagabati A.K. (2023): Dendrochronology in the tropics using tree-rings of *Pinus kesiya*. Dendrochronologia, 78: 126070.

Trisurat Y., Kanchanasaka B., Kreft H. (2015): Assessing potential effects of land use and climate change on mammal distributions in northern Thailand. Wildlife Research, 41: 522–536.

Vacek Z., Vacek S., Cukor J. (2023). European forests under global climate change: Review of tree growth processes, crises and management strategies. Journal of Environmental Management, 332: 117353.

Wigley T.M.L., Briffa K.R., Jones P.D. (1984): On the average value of correlated time series, with applications in dendroclimatology and hydrometeorology. Journal of Applied Meteorology and Climatology, 23: 201–213.

Received: November 4, 2025
Accepted: March 18, 2026
Published online: April 17, 2026